Pergamon

Int. J. Solids Structures Vol. 32, No. 6/7, pp. 897–909, 1995

0020-7683/95 $9.50 + .00

0020-7683(94)00167-7

ON IMPROVEMENTS IN MEASURING CRACK ARREST TOUGHNESS

ROBERT J. BONENBERGER and JAMES W. DALLY
Mechanical Engineering Department, University of Maryland, College Park, MD 20742, U.S.A.

(*Received* 21 *December* 1993; *in revised form* 22 *April* 1994)

Abstract—A new specimen is described for determining fracture toughness of metals in a more cost effective manner. The chevron-notched crack arrest (CNCA) specimen is a hybrid design which allows measurement of K_{Ia} and K_{Ic} from a single specimen. Both finite element analyses and a compliance experiment are used to relate K to strains and crack mouth opening, as measured by strain and clip gages, respectively. Fracture experiments using the CNCA specimen on A533-B reactor grade steel are discussed.

INTRODUCTION

The behavior of a structure with a serious flaw or crack is usually predicted with a fracture mechanics analysis that employs some measure of the crack initiation toughness. If the structure is operating at or near the lower shelf of the brittle to ductile transition, the plastic zone prior to initiation is very small and the static initiation toughness K_{Ic}, as measured in accordance with ASTM E399-90 (1993), is the controlling property. However, if the structure is operating near the upper shelf, the initiation toughness is expressed in terms of the J integral. The material property in this instance is J_{Ic}, measured in accordance with ASTM E813-89 (1993). The J_{Ic} values can be converted to their equivalent in terms of stress intensity factor, which is denoted K_{Jc}. In both of these cases, crack initiation under plane strain conditions is initiated when

$$K_I \geqslant K_{Ic} \tag{1}$$

$$K_J \geqslant K_{Jc}. \tag{2}$$

While these equations are similar, they predict different crack growth behavior; eqn (1) describes the onset of high velocity cleavage and eqn (2) describes initiation of stable, low velocity tearing.

This paper is concerned with high velocity cleavage and, although the stress state is static prior to initiation, the propagation behavior of the crack is clearly controlled by dynamic states of stress. In dynamic photoelastic experiments conducted over a decade ago, Dally (1981) and associates (Kobayashi and Dally, 1977; Irwin *et al.*, 1979) determined a relation between the propagation toughness K_{ID} and the crack tip velocity $\dot{a}$, as shown in Fig. 1, for a brittle polymer known commercially as Homalite 100. While the uniqueness of the K_{ID}–$\dot{a}$ relationship has been a controversial topic (Ravi-Chandar and Knauss, 1984; Dally *et al.*, 1985), its existence has been accepted provided that K and $\dot{a}$ are averaged both spatially and temporally. Indeed, curves describing the K_{ID}–$\dot{a}$ relation for steels show similar characteristics, although Kobayashi and Dally (1980) found the scatter in experimental results to be much larger than that observed in brittle polymers.

The K_{ID}–$\dot{a}$ relationship, as depicted in Fig. 1, illustrates three important features of crack propagation. First there is a terminal velocity that is usually much less than the Rayleigh wave velocity c_R, which is the theoretical maximum. The second important feature is branching, which occurs when the crack is over driven. The fracture process zone becomes larger and micro-cracks form at angles to the main crack path, which causes surface roughening. The crack systems compete and when the driving stress intensity K_I becomes

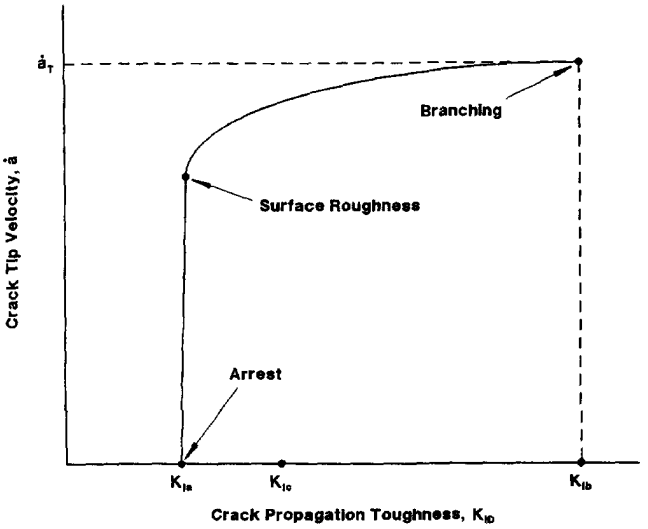

Fig. 1. K_{ID}–$\dot{a}$ relation characterizing the dynamic behavior of a propagating crack.

sufficiently large, one or more off-axis groupings of cracks dominate and the crack multiplies into two or more branches (Shukla *et al.*, 1987).

The third feature is arrest. When the driving stress intensity K_I drops below some critical value defined as the arrest toughness K_{Ia}, the crack velocity abruptly decreases to zero (Crosley and Ripling, 1980). Crack arrest toughness is important because it represents a lower-bound toughness for *static* crack initiation. This fact is evident by the relative positions of K_{Ia} and K_{Ic} in Fig. 1. The amount of scatter in measurements of the crack initiation toughness is enormous, as indicated in Fig. 2 (Link and Joyce, 1994). The magnitude of the scatter (several hundred percent) is not well recognized, and often those responsible for fracture mechanics analysis use average values or handbook values for crack initiation toughness. The result is an embarrassing continuation of field failures that have led Rosenfield and Marschall (1992) to unfortunately conclude that "no significant improvements in the accuracy of fracture-mechanics analysis of structural failures over the past twelve years have been made."

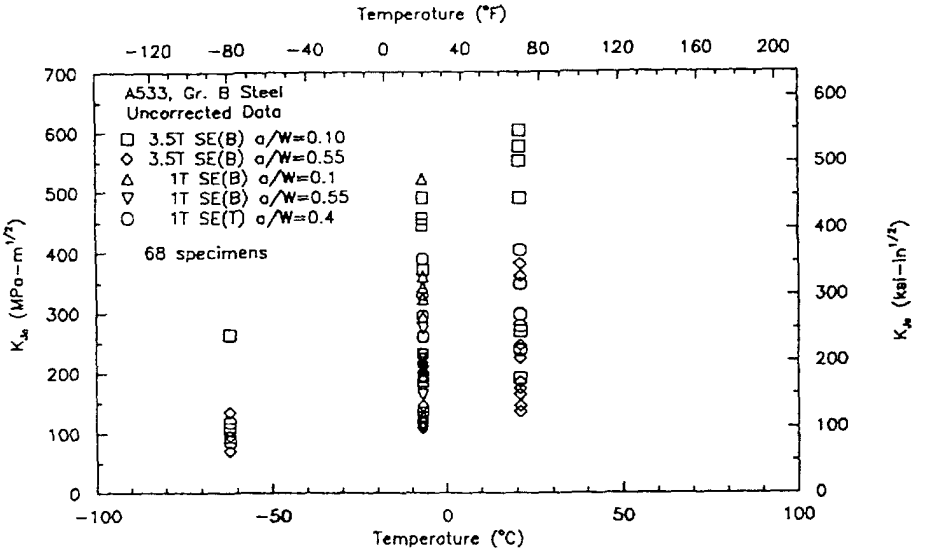

Fig. 2. Large amounts of scatter occurs in measurements of fracture toughness K_{Jc} over the temperature transition range [from Link and Joyce (1994)]. Copyright ASTM. Reprinted with permission.

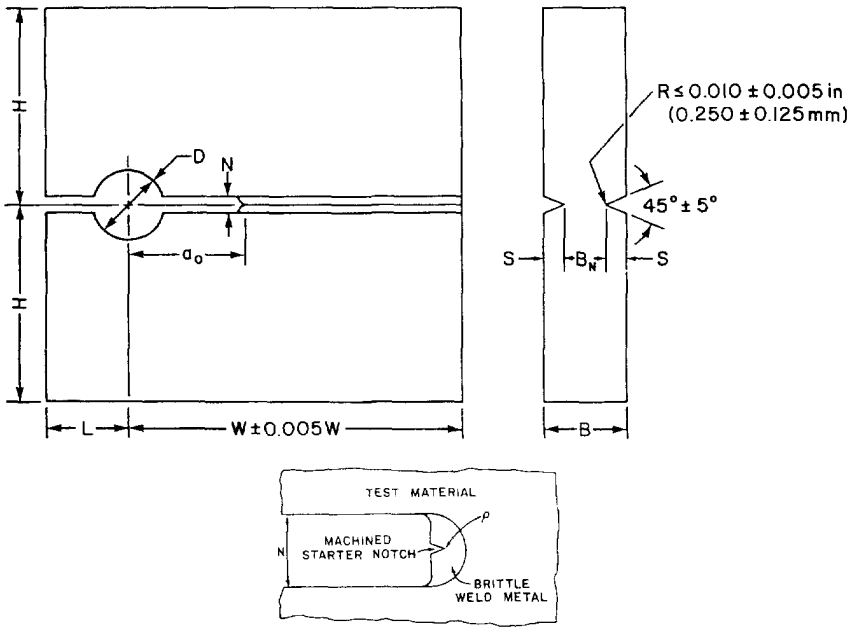

Fig. 3. Geometry and dimensions of a crack-line wedge-loaded compact crack arrest specimen [from ASTM E1221 (1993)]. Copyright ASTM. Reprinted with permission.

To design and analyse safe structures, the very significant scatter in crack initiation toughness must be recognized. For conservative design, it is mandatory that the lower-bound toughness be employed in fracture mechanics analysis. It appears that measurements of crack arrest toughness may provide a more effective and more economical means of estimating lower-bound toughness. Also, the scatter in the measurement of K_{Ia} is significantly less than the scatter encountered in measuring K_{Ic}.

DETERMINING CRACK ARREST TOUGHNESS CURRENTLY

The standard method for measuring crack arrest toughness is described in ASTM E1221-88 (1993). The specimen employed (see Fig. 3) is similar to a compact tension specimen except for the loading hole and the notch tip geometry. The crack tip is prepared by placing a bead of brittle weld metal at the end of the slot and then machining a starter notch into the weld, as indicated in Fig. 3. Crack-line loading is accomplished by driving a wedge through a top-flanged, split D pin, as shown in Fig. 4. The loading is cycled by inserting and withdrawing the wedge until crack initiation occurs. The running crack propagates into a decreasing K-field, which causes the crack to slow and eventually arrest.

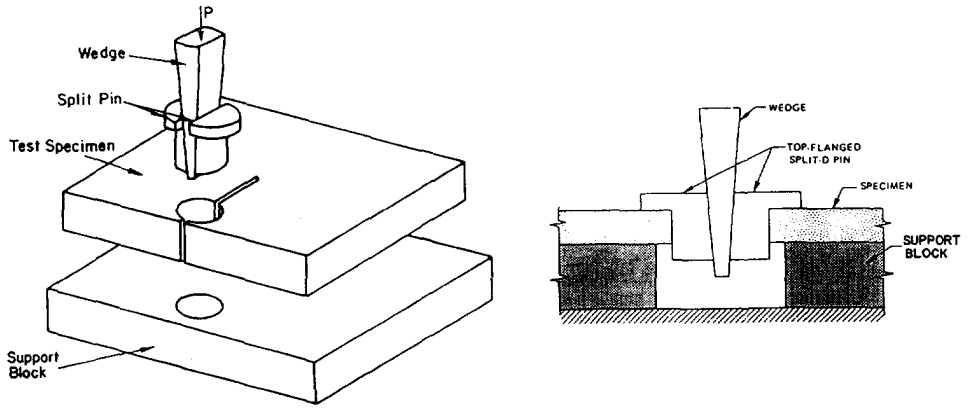

Fig. 4. Standard arrangement for applying the crack-line load with a transverse wedging action [from ASTM E1221 (1993)]. Copyright ASTM. Reprinted with permission.

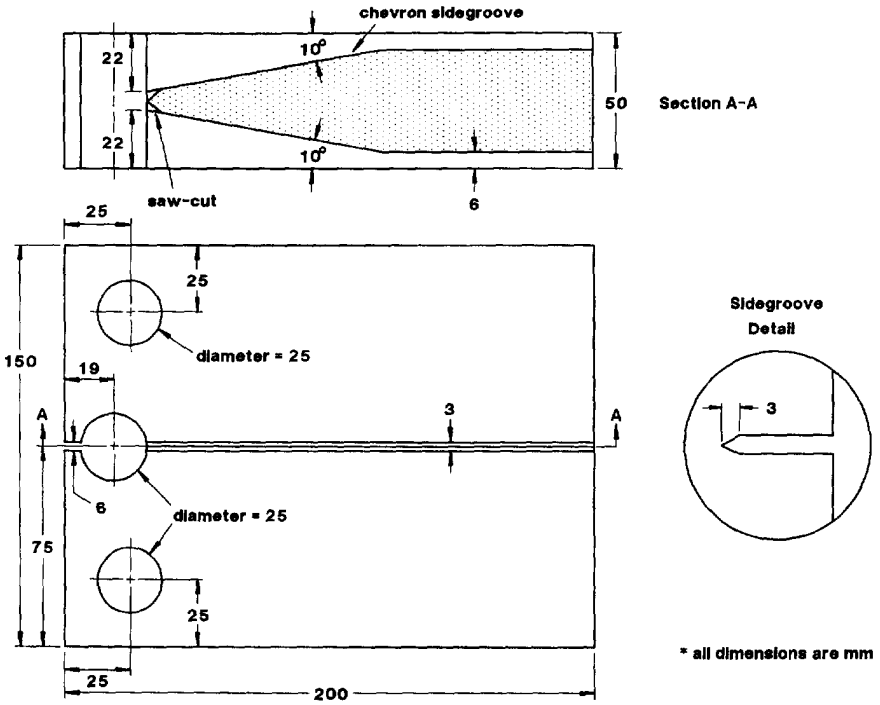

Fig. 5. The proposed arrest/initiation specimen.

The arrest toughness is determined from the crack mouth opening displacement and the length of the arrested crack (a_a) using a static, K-based analysis.

Measurement of the arrest toughness K_{Ia} following the procedures in E1221 is difficult, time consuming and costly. The specimen is large for typical engineering steels in the low to middle strength range. Also, placement of the brittle weld metal is an art that is not found in the ordinary materials laboratory. Fatigue cycling with a wedge to condition the crack tip is awkward and time consuming. Finally, the number of invalid tests is large because one or more of the test conditions were not satisfied. In the round robin tests that were conducted prior to the adoption of E1221, only 45% of the tests performed were considered valid even though the test conditions were closely controlled (Barker *et al.*, 1988). Reasons for invalid results include failure of the crack to initiate or arrest, a crack jump that was either too short or too long, or unusual features on the fracture surfaces such as tunnelling, large remaining ligaments, or propagation out of the side-groove plane. Despite the low success rate, the K_{Ia} data gave a coefficient of variation of 0.118, which was modest when compared to that encountered in K_{Ic} testing (see Fig. 2).

IMPROVING THE MEASUREMENT METHOD

To improve the method for measuring K_{Ia}, it is desirable to reduce the specimen size, to eliminate the brittle weld metal, and to increase the probability of a valid test. These improvements were made possible by designing a new crack arrest specimen incorporating a chevron notch. A second objective of this program was to measure a second property from the same specimen, namely the crack initiation toughness K_{Ic} from the arrested crack. This dual usage of the new CNCA (chevron-notched crack arrest) specimen enhances its cost effectiveness by providing two measurements of properties that are important in the fracture mechanics analysis of structures fabricated from typical engineering steels.

The specimen geometry is presented in Fig. 5. The hole on the center line is to accommodate a transverse wedge for crack-line loading. The other two holes are for pins used to apply in-plane tensile loading. A thin slot 3 mm wide is cut into the center line to form a chevron-style side-groove. The chevron has an included angle of 20° and is shown clearly on the sectional view of the crack plane. Note that the shaded region represents the

uncut material in the crack plane. The slot is finished with a V-notched cutting tool that has a 45° included angle to give the side-groove a sharply configured bottom (see Fig. 5).

The specimen is pin loaded in cyclic tension to form a fatigue sharpened crack tip, as illustrated in Fig. 6. The crack front is parabolic in shape due to the influence of the sharp-bottomed chevron side-groove. This shape is advantageous because it essentially lengthens the crack, thereby increasing the probability of locating a cleavage initiation site very near the crack front.

The CNCA specimen is next loaded with a transverse wedge using the same arrangement as in E1221 (see Fig. 4). The load on the wedge is increased monotonically until the crack initiates. As the crack propagates, the resistance to fracture increases because the thickness B_N of the chevron is increasing. Also with crack-line loading, the crack is propagating into a decreasing K-field. Both of these features promote crack arrest. A typical first arrest is evident in the photograph of the fracture surface shown in Fig. 6. The length of the crack jump (Δa) is variable from test to test, even with the same material. The crack jump distance increases as the difference between the initiation toughness and the arrest toughness increases.

The arrest location is marked either by heat tinting or by the application of a dye penetrant. The specimen is then reloaded a second time to induce another initiation, using the arrested crack as the initial crack tip condition. The loading can be applied at the crack line with the wedge or externally with separating forces applied by pins.

The CNCA specimen is instrumented with a clip gage to measure crack mouth opening displacement and with strain gages located on the top edge of the specimen, as shown in Fig. 7. The clip gage signal is monitored on an x–y recorder, and the strain gage signals are stored on a digital oscilloscope.

SPECIMEN DYNAMICS

While the crack run–arrest event is a dynamic event, the method employed in E1221 to determine K_{Ia} is based on a static analysis. This use of a static analysis was justified only because the dynamic effects were small. Since static analysis methods (described later) are used in the development of the new CNCA specimen, it is essential to show the magnitude of any dynamic effect that will influence the interpretation of the experimental data.

A typical strain–time trace for a load–run–arrest event is shown in Fig. 8(a). As the wedge was driven into the split D pin, the compressive strain sensed by the strain gages increased monotonically until the crack initiated at time $t = 110$ s. The strains decreased abruptly as the crack jumped about 66 mm before arresting. An expanded time view of the strain gage response during the propagation and arrest period is given in Fig. 8(b). The run–arrest occurred in about 80 μs. The specimen arms then oscillated at a frequency of about 12.5 kHz with some damping for about 1 ms. The amplitude of the oscillation was only 8% of the steady-state strain difference between initiation and arrest. The oscillation is due to the transfer of strain energy in the specimen, which existed during propagation, to kinetic energy of the vibrating arms immediately following arrest. The steady-state value of the strain represents the best estimate of the far-field strain at the instant of arrest.

The magnitude of the oscillation increases with the crack jump distance and the length of the arms. An 8% oscillation occurred with a crack jump distance of 66 mm, with specimen arms that were 118 mm at arrest. While our experience in testing is limited to a few specimens, we believe that the amplitude of the oscillations will usually be within the 5–12% range. For this reason, the influence of specimen dynamics was neglected in the subsequent analyses performed to calibrate the CNCA specimen.

SPECIMEN CALIBRATION

The CNCA specimen was calibrated using two independent methods, namely finite element analysis and compliance measurements. Both methods assumed linear elastic behavior and considered the specimen as a two-dimensional body in plane stress. The finite element modeling employed 12-node isoparametric elements. The model also incorporated

an enriched crack tip element with a singular ($r^{1/2}$) displacement field corresponding to the plane stress solution for the mode I stress intensity factor (Gifford, 1991). A total of 79 elements were employed in the model, as indicated in Fig. 9. A series of point loads totaling 4500 N were applied to the central hole using the conventional cosine distribution to model the bearing of the split D pins against the CNCA specimen. The solution provided by the finite element analysis, for crack lengths from 56 to 144 mm, included the strain distribution along the top edge of the specimen, the crack mouth opening displacement, and the stress intensity factor K_I. The results of the numerical analysis are shown together with the experimental findings in Figs 10 and 11.

To perform the compliance calibration, following a method employed by Crosley and Ripling (1981), a full scale model of the CNCA specimen was machined from 6061-T6 aluminum. The specimen was instrumented with 20 strain gages positioned along the top edge and with a clip gage located at the crack mouth. Because of friction effects and uncertainties in the applied loads, the transverse wedge could not be used in the compliance experiments to apply the loading at the central hole. Instead, a split pin with a clevis arrangement was employed that permitted crack-line loading to be applied (and accurately measured) with a servo-controlled, hydraulically actuated universal testing machine. For each crack length, the specimen was loaded in eight increments and measurements of the strains and crack mouth opening displacement were made. The crack was extended from 56 to 144 mm in 12.5 mm increments, and the compliance measurements were repeated for each crack length.

The results for the strain distribution along the top edge of the specimen are shown in Fig. 10. The lines give the results of the finite element analyses, and the symbols show the results from the strain gage measurements made in the compliance experiments. Clearly, the numerical analysis and the experimental results compare very closely.

The results for the crack mouth opening displacement v from the two different methods are presented in Fig. 11. Again the comparison is good, particularly for the short to medium length cracks. Some differences are observed for the longer cracks, with the compliance measurement giving slightly larger displacements. This difference is probably due to the material removed in machining the 3 mm slot for the side-groove, which reduced the rigidity of the arms of the specimen. The loss of the material due to the slot was not considered in the two-dimensional finite element model.

The final comparison of the stress intensity factor K_I from the two methods is presented in Table 1, where the proportionality constant $\alpha = K_I/v$ is given as a function of crack length a. In determining the stress intensity factor K_I from the output of the finite element program and from the compliance experiment, it was necessary to correct for the variable thickness B_N. Due to the chevron notch, B_N varies with the crack length. The standard correction procedure that is used when the thickness change is modest along the direction of crack propagation (Kobayashi and Dally, 1980) gives

$$(K_I)_G = (B/B_N)^{1/2}(K_I)_P \tag{3}$$

where B is the thickness of the CNCA specimen, B_N is the net thickness, G identifies the side-grooved specimen and P identifies a plane model. This adjustment has been employed in generating Table 1.

Determination of K_{Ia} and K_{Ic} is straightforward. The crack length a at arrest or reinitiation is measured, and the corresponding α is selected from Table 1, interpolating if necessary. The fracture toughness can then be calculated from the following relations:

$$K_{Ia} = \alpha v_a \tag{4}$$

$$K_{Ic} = \alpha v_c \tag{5}$$

where v_a and v_c are the crack mouth opening displacements at arrest and initiation, respectively, as measured by the clip gage. A similar procedure is employed to determine K_{Ia} and K_{Ic} from the strain gage data.

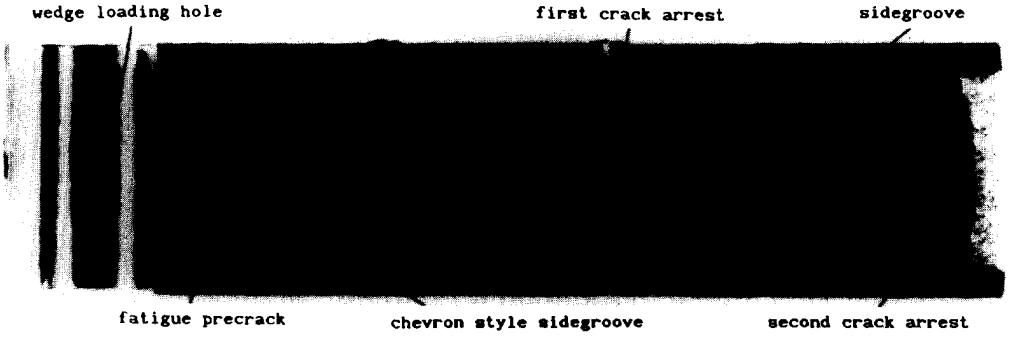

Fig. 6. Typical fracture surface.

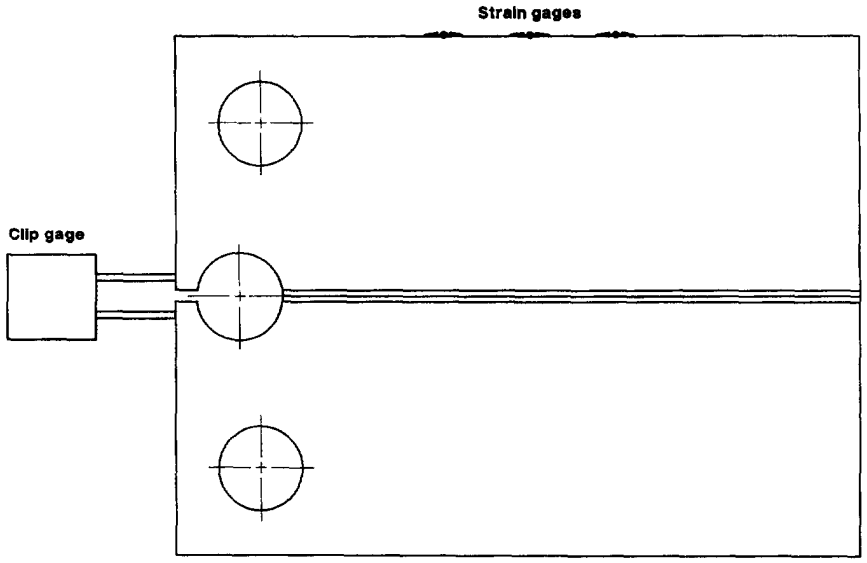

Fig. 7. Instrumented CNCA specimen.

RESULTS

Four experiments have been conducted using the CNCA specimen to measure both K_{Ia} (the arrest toughness) and K_{Ic} (the reinitiation toughness). The specimens were machined from A533-B reactor grade steel with well known properties (Barker *et al.*, 1988). The yield strength of the steel was 480 MPa and its reference nil-ductility temperature (RT_{NDT}) was $-2°C$. Two separate experiments were conducted with each specimen, the first to measure K_{Ia} and the second to measure K_{Ic} (reinitiation).

The results for the crack arrest experiments are presented in Table 2. All four experiments initiated successfully, and the crack arrested near the central region of the specimens. The average value of K_{Ia} for all tests was 101.5 MPa-m$^{1/2}$. As expected, the crack jump distance varied significantly because of the specimen to specimen scatter in K_{Ic}. There was a difference in the results for K_{Ia} using the data from the clip gage and the data from the strain gages that must be attributed to accumulated experimental error. The maximum difference, which occurred with specimen C, was 6.3%, although the average error was much lower. The results for K_{Ia} exhibited specimen to specimen variation as expected. A sample size of four is very small for confidence in a statistical analysis, although the coefficient of variation was computed as 0.148.

The results for measurements of the crack initiation toughness from a previously arrested crack are presented in Table 3. Three of the four specimens reinitiated, giving an average value of K_{Ic} of 238.9 MPa-m$^{1/2}$. The crack did not initiate in one case, even though the specimen was loaded to its limit ($K_I > 300$ MPa-m$^{1/2}$ for the arrested crack length) where plastic effects become dominant. Comparison of these results with those presented by Link and Joyce (1994) in Fig. 2 shows that measurements of K_{Ic} fall in the lower range of the expected values for A533-B reactor grade steel.

DISCUSSION AND CONCLUSIONS

Crack arrest toughness K_{Ia} is an important property because of its value in predicting structural performance in a fracture mechanics analysis. Arrest toughness can be employed to determine if a crack propagating in a decreasing K-field will arrest. Arrest toughness is also an excellent estimate of the lower bound for the crack initiation toughness. As such, K_{Ia} is useful in conservative predictions of crack instability in statically loaded structures. Because the scatter in measurements of K_{Ia} are much smaller than the scatter in measurements of K_{Ic}, it is probably more economical to estimate the lower-bound initiation toughness by determining K_{Ia} rather than K_{Ic}.

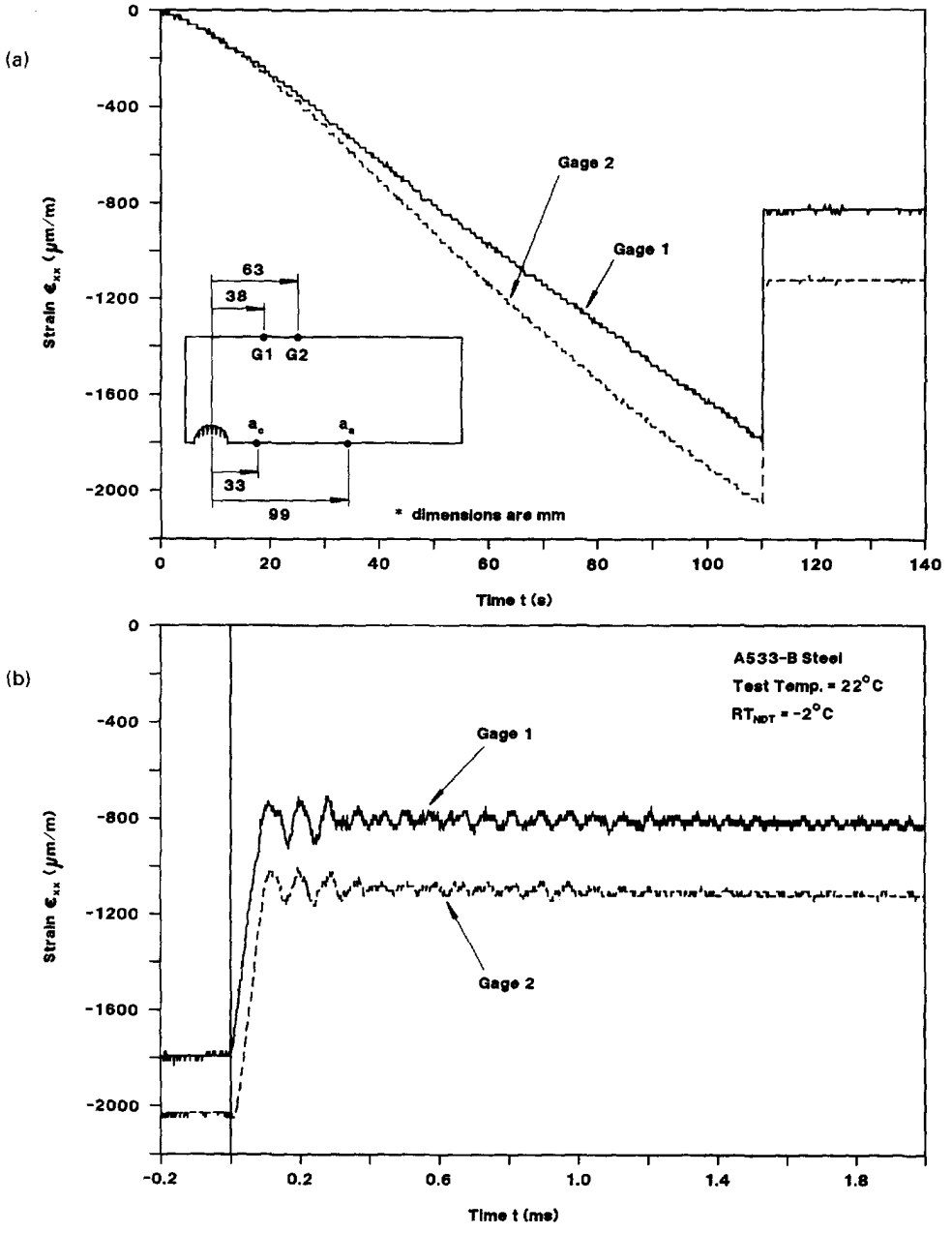

Fig. 8 (a). Typical strain gage records of a run–arrest event; (b) dynamic features of a run–arrest event.

Table 1. Proportionality constant $\alpha = K_I/v$

Crack length a (mm)	Constant α (GPa/m$^{1/2}$) FEM	Compliance
56	366.0	324.5
69	280.9	263.0
81	223.7	211.7
94	184.0	170.6
106	159.9	151.6
119	147.3	137.3
131	136.9	121.8
144	124.9	113.0

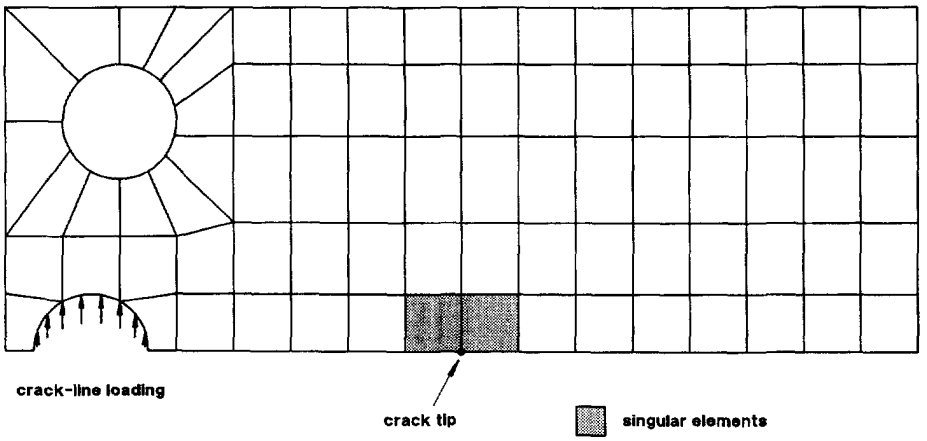

Fig. 9. The finite element model.

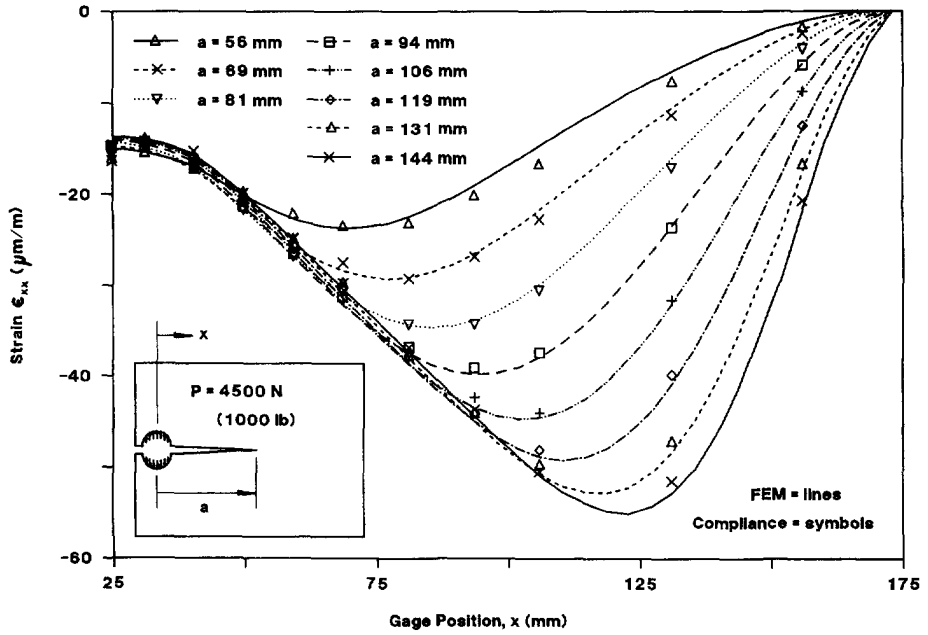

Fig. 10. Comparison of strains from the finite element analysis and the compliance experiments.

The current ASTM standard procedure for measuring K_{Ia} (E1221) specifies a test that is difficult to conduct and prone to failure. This paper describes a modified specimen and test procedure intended to improve on E1221. The modified procedure retains the transverse wedge for crack-line loading but eliminates the brittle weld material and the starter notch. In the modified CNCA specimen, the initiation is from a fatigue sharpened crack with a relatively long crack front. After initiation, crack arrest is ensured, with a reasonable crack

Table 2. Crack arrest toughness K_{Ia} from arrest experiments

Specimen	Δa (mm)	B_N† (mm)	K_{Ia} (MPa-m$^{1/2}$) Clip gage	Strain gage	Average
A	58	34	102.0	94.0	98.0
B	48	27	104.8	108.3	106.6
C	67	37	111.1	126.0	118.6
D	59	32	83.1	82.7	82.9
				Grand average =	101.5

Δa = crack jump distance
† B_N at the arrest location.

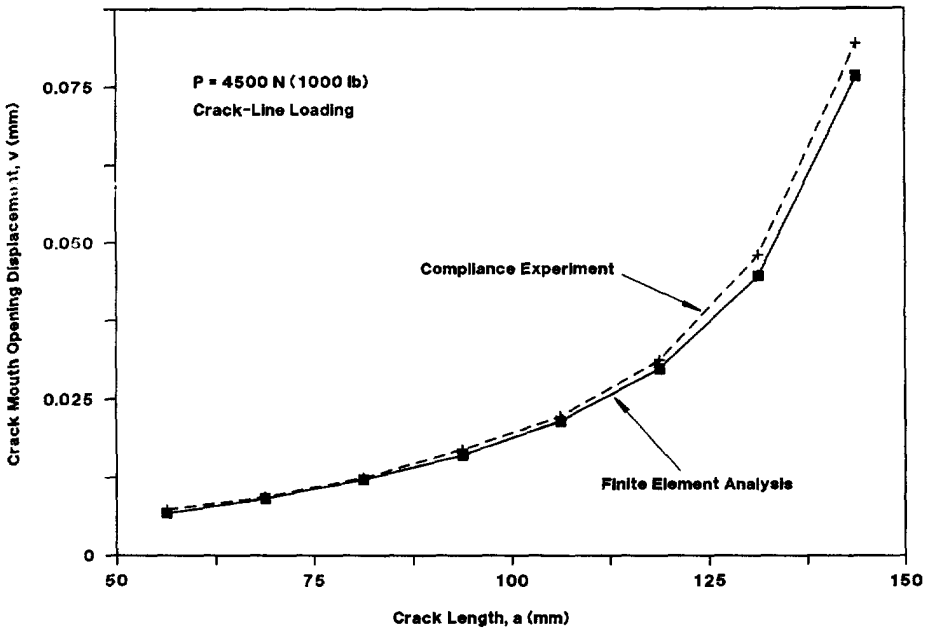

Fig. 11. Comparison of crack mouth opening displacement from the finite element analysis and the compliance experiments.

Table 3. Crack initiation toughness K_{Ic} from reinitiation experiments

Specimen	a/W	B_N† (mm)	K_{Ic} (MPa-m$^{1/2}$) Clip gage	Strain gage	Average
A	0.497	34	208.7	175.9	192.3
B	0.381	27	305.8	280.0	292.9
C	0.547	37	243.3	219.9	231.6
D	0.457	32	‡	‡	‡
				Grand average =	238.9

† B_N at the reinitiation location
‡ Plastic bending occurred before cleavage initiation, $K_{Ic} > 300$ MPa-m$^{1/2}$.

jump distance, by employing a chevron notch that permits B_N and the fracture resistance to increase while the K-field decreases.

Following the measurement of K_{Ia}, the CNCA specimen is employed in a second experiment to measure the crack initiation toughness from the arrested crack. Thus, the specimen and the procedure provides for both arrest and initiation toughness data.

While the preliminary experiments with A533-B reactor grade steel have been limited, the results show that the procedure is reliable (four specimens all initiated and yielded valid K_{Ia} measurements). The results for arrest toughness appear to be consistent with those measured during the round robin tests performed in the development of the E1221 standard.

Acknowledgements—The authors greatly appreciate the advice received from Professors G. R. Irwin and W. L. Fourney over the course of this investigation. Thanks are also due to the Oak Ridge National Laboratory and the National Science Foundation for the financial support of our research programs.

REFERENCES

ASTM E399-90 (1993). Plane-strain fracture toughness of metallic materials. *Annual Book of ASTM Standards*, Vol. 03.01. ASTM, Philadelphia, PA.

ASTM E813-89 (1993). J_{Ic}, a measure of fracture toughness. *Annual Book of ASTM Standards*, Vol. 03.01. ASTM, Philadelphia, PA.

ASTM E1221-88 (1993). Determining plane-strain crack-arrest fracture toughness, K_{Ia}, of ferritic steels. *Annual Book of ASTM Standards*, Vol. 03.01. ASTM, Philadelphia, PA.

Barker, D. B., Chona, R., Fourney, W. L. and Irwin, G. R. (1988). A report on the round robin program conducted to evaluate the proposed ASTM standard test method for determining the plane strain crack arrest

fracture toughness, K_{Ia}, of ferritic materials. USNRC Report NUREG/CR-4996 (ORNL/SUB/79-7778/4). University of Maryland, College Park, MD.

Crosley, P. B. and Ripling, E. J. (1980). Significance of crack arrest toughness (K_{Ia}) testing. In *ASTM STP* 711 (Edited by G. Hahn and M. Kanninen), pp. 321–337. ASTM, Philadelphia, PA.

Crosley, P. B. and Ripling, E. J. (1981). Development of a standard test for measuring K_{Ia} with a modified compact specimen. USNRC Report NUREG/CR-2294 (ORNL/Sub-81/7755/1). Materials Research Laboratory, Glenwood, IL.

Dally, J. W. (1981). Developments in photoelastic analysis of dynamic fracture. In *Proc. IUTAM Symp. Optical Meth. Mech. Solids* (Edited by A. Lagarde), pp. 359–394. Sijthoff and Noordhoff, Rockville, MD.

Dally, J. W., Fourney, W. L. and Irwin, G. R. (1985). On the uniqueness of the stress intensity factor–crack velocity relationship. *Int. J. Fract.* **27,** 159–168.

Gifford, L. N. (1991). Documentation of PC APES fracture and stress analysis. David Taylor Research Center Report DTRC-SSPD-91-172-39. David Taylor Research Center, Bethesda, MD.

Irwin, G. R., Dally, J. W., Kobayashi, T., Fourney, W. L., Etheridge, M. J. and Rossmanith, H. P. (1979). On the determination of the $\dot{a}$–K relationship for birefringent polymers. *Expl Mech.* **19,** 121–128.

Kobayashi, T. and Dally, J. W. (1977). Relation between crack velocity and the stress intensity factor in birefringent polymers. In *ASTM STP* 627 (Edited by G. Hahn and M. Kanninen), pp. 257–273. ASTM, Philadelphia, PA.

Kobayashi, T. and Dally, J. W. (1980). Dynamic photoelastic determination of the $\dot{a}$–K relation for 4340 alloy steel. In *ASTM STP* 711 (Edited by G. Hahn and M. Kanninen), pp. 189–210. ASTM, Philadelphia, PA.

Link, R. E. and Joyce, J. A. (1994). Experimental investigation of fracture toughness scaling models. To appear in *ASTM STP* 1244 (Edited by M. Kirk and A. Bakker). ASTM, Philadelphia, PA.

Ravi-Chandar, K. and Knauss, W. G. (1984). An experimental investigation into dynamic fracture: III. On steady-state crack propagation and crack branching. *Int. J. Fract.* **26,** 141–154.

Rosenfield, A. R. and Marschall, C. W. (1992). Fracture-mechanics-based failure analysis. USNRC Report NUREG/CR-5860 (ORNL/SUB/82-17624/1). Battelle, Columbus, OH.

Shukla, A., Zervas, H. and Nigam, H. (1987). A critical review of dynamic crack branching criteria. In *Proc.* 1987 *SEM Fall Conf. Dynamic Failure*, pp. 80–85. SEM, Bethel, CT.